J. Fluid Mech. (1997), *vol.* 332, *pp.* 377–394
Copyright © 1997 Cambridge University Press

Towards the concept of hydrodynamic cavitation control

By DHIMAN CHATTERJEE AND VIJAY H. ARAKERI

Department of Mechanical Engineering, Indian Institute of Science, Bangalore 560012, India

(Received 22 January 1996 and in revised form 28 August 1996)

A careful study of the existing literature available in the field of cavitation reveals the potential of ultrasonics as a tool for controlling and, if possible, eliminating certain types of hydrodynamic cavitation through the manipulation of nuclei size present in a flow. A glass venturi is taken to be an ideal device to study the cavitation phenomenon at its throat and its potential control. A piezoelectric transducer, driven at the crystal resonant frequency, is used to generate an acoustic pressure field and is termed an 'ultrasonic nuclei manipulator (UNM)'. Electrolysis bubbles serve as artificial nuclei to produce travelling bubble cavitation at the venturi throat in the absence of a UNM but this cavitation is completely eliminated when a UNM is operative. This is made possible because the nuclei, which pass through the acoustic field first, cavitate, collapse violently and perhaps fragment and go into dissolution before reaching the venturi throat. Thus, the potential nuclei for travelling bubble cavitation at the venturi throat seem to be systematically destroyed through acoustic cavitation near the UNM. From the solution to the bubble dynamics equation, it has been shown that the potential energy of a bubble at its maximum radius due to an acoustic field is negligible compared to that for the hydrodynamic field. Hence, even though the control of hydrodynamic *macro* cavitation achieved in this way is at the expense of acoustic *micro* cavitation, it can still be considered to be a significant gain. These are some of the first results in this direction.

1. Introduction

Cavitation in liquids is the formation and subsequent dynamic life of bubbles in liquids subjected to a sufficiently low pressure. These bubbles can be either gas or vapour filled and can occur in a variety of liquids under a wide range of conditions. The required low pressure can be created either by an imposed acoustic field produced by a piezoelectric or magnetostrictive transducer or due to flow of a liquid through a constricted passage as in a venturi throat. Depending upon the origin, cavitation is termed as acoustic or hydrodynamic. It has now been well established that cavitation originates from weak spots commonly termed 'nuclei' which exist in the liquid. A simple model for these nuclei is microscopic voids with some vapour and dissolved gases contained in them. Understanding the role of nuclei is one of the central problems in cavitation research and has been discussed by many investigators, for example Flynn (1964) for acoustic cavitation and Holl (1970) for hydrodynamic cavitation. One significant point to be noted in this connection is that for most types of hydrodynamic cavitation, a continuous supply of nuclei is required, whereas for acoustic cavitation, the liquid sample is stagnant and there is replenishment

https://doi.org/10.1017/S0022112096004223 Published online by Cambridge University Press

of nuclei by a mechanism to be discussed later on. In view of this, there have been considerable efforts to measure nuclei size and distribution for hydrodynamic cavitation, Billet (1986).

Acoustic cavitation has been the subject of considerable research in the past. In the present context, the significant aspects were attempts to measure tensile strengths of liquid samples and the possible different types of cavity motions. Following Flynn (1964), the following types of cavity motions can be identified which are consistent with experimental observations: *stable cavity* if it oscillates nonlinearly about its equilibrium radius; *transient cavity* if, on contraction from some maximum size, its initial motion approximates that of a Rayleigh cavity and is followed by a violent collapse.

Further, based on computations of cavity motions, Flynn has suggested that in the case of transient cavity motion, the bubbles expand to a maximum radius of about two to three times the initial radius. Other criteria have also been suggested by Apfel (1981) and Arakeri & Chakraborty (1990). Transient cavities can be formed in a single acoustic cycle and are termed by Flynn & Church (1988) 'prompt transient cavities'; stable nuclei may also exhibit transient motion after a few cycles. In fact, for nonlinear bubble motion, there will be a size distribution of nuclei that can grow into transient cavities for a given combination of frequency and pressure amplitude.

The most interesting part of the transient cavity motion is its collapse phase. Flynn & Church (1984) have postulated that when a transient cavity implodes, it may rebound or it may fragment into several smaller gas bubbles. Later, Flynn & Church (1988) have pointed out that the interface of a collapsing bubble is inherently unstable and the collapsing bubbles may deform and disintegrate. This can lead to proliferation of nuclei, the majority of which are unstable to mass diffusion so that only a few may survive and act as sites for subsequent transient cavity motions. The time period of their survival can be obtained from mass diffusion equations, as done by Epstein & Plesset (1950). Based on this and some hypotheses on the number and size of nuclei generated from a transient cavity, Flynn & Church (1988) have explained the observed maxima in iodine release with different acoustic pressure field pulse durations.

Two experiments are worth mentioning in connection with the fragmentation of transient cavities. Nyborg & Hughes (1967) have observed the phenomenon of 'bubble annihilation' in an acoustic field produced by a magnetostrictive transducer in a vessel with transparent walls. In an another experiment Harrison (1952) has reported the phenomenon of bubble disappearance in hydrodynamic cavitation in a venturi. A finding which can be related to the possibility of fragmentation of a transient cavity into a large number of smaller ones is the observation of Barger (1964), who found that certain types of nuclei can be destroyed by repeated cavitation. Using the concept of collapse and fragmentation of transient cavities and their subsequent dissolution, Arakeri & Chakraborty (1990) proposed the use of ultrasonics for hydrodynamic cavitation control.

In contrast to acoustic cavitation, hydrodynamic cavitation originates from the flow of liquids past a solid object or in a constricted passage when the local pressure falls below the critical pressure. Following Knapp, Daily & Hammitt (1970), three primary types of hydrodynamic cavitation can be identified: travelling bubble cavitation, fixed or attached cavitation, and vortex cavitation. In applied hydrodynamics, effects due to cavitation, like the loss in performance of hydraulic machinery, material erosion and surface damage, cavitation-induced noise and vibration are mostly undesirable. Even though a significant extent of cavitation is required to observe some of these

https://doi.org/10.1017/S0022112096004223 Published online by Cambridge University Press

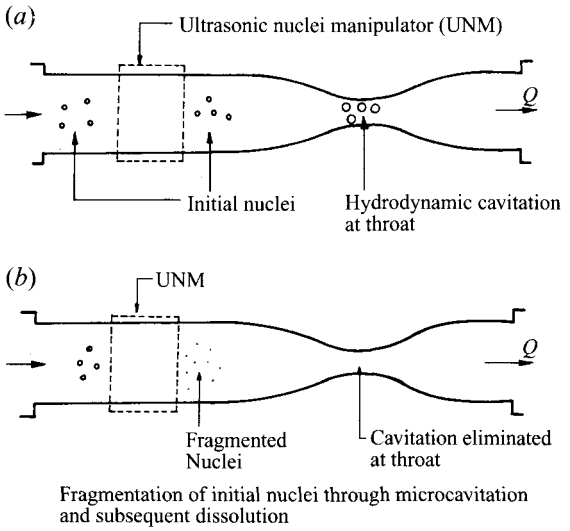


FIGURE 1. Schematic diagram of the proposed experimental set-up with the ultrasonic nuclei manipulator (UNM) (*a*) inoperative and (*b*) operative, and the expected results.

effects, there are situations like submarine propellers where even a small amount of cavitation is undesirable.

The above problems with hydrodynamic cavitation make it imperative to control it. To the best of our knowledge, even though considerable efforts have been expended in trying to understand the conditions for the onset of hydrodynamic cavitation, relatively few efforts have been devoted to devise means of controlling or eliminating it. In one such attempt, as indicated earlier, Arakeri & Chakraborty (1990) have suggested the potential use of ultrasonics but their proposals are yet to be tested experimentally. The present work aims at towards remedying this.

The set-up of the present work is as suggested by Arakeri & Chakraborty (1990) and is illustrated schematically in figure 1. As hydrodynamic cavitation, unlike acoustic cavitation, requires a continuous supply of nuclei for its sustenance, an ultrasonic piezoelectric transducer, termed a UNM (ultrasonic nuclei manipulator), is installed to control the number of nuclei reaching the hydrodynamic low-pressure region. In the absence of the UNM, on reaching the venturi throat the nuclei can grow and collapse violently. If the UNM is made operative, it is expected that the nuclei will be destroyed in the acoustic field set up by the UNM through mechanisms discussed above and cavitation can be prevented at the venturi throat. As this experiment depends on a copious supply of nuclei, electrolysis is used for this purpose upstream of the UNM. The experimental set-up required to achieve our objectives is described next. This is followed by a presentation of results and discussion and finally a summary is provided.

2. Experimental set-up

Figure 2 shows a schematic of the overall set-up. Two large inlet tanks of capacity 20 l each were connected in series and this helped to maintain an almost constant head during each run. An exhaust glass tank, also having a capacity of 20 l, is placed on a laboratory-made weighing machine and connected to a metallic vacuum tank and a vacuum pump in series. The insertion of a vacuum tank in between the

https://doi.org/10.1017/S0022112096004223 Published online by Cambridge University Press

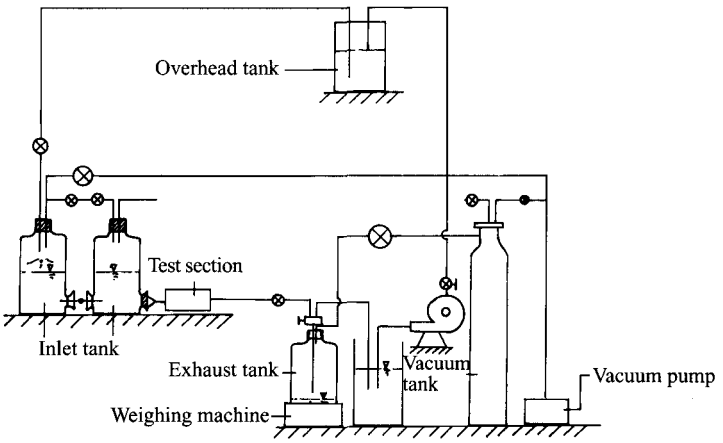


FIGURE 2. Schematic of the experimental set-up.

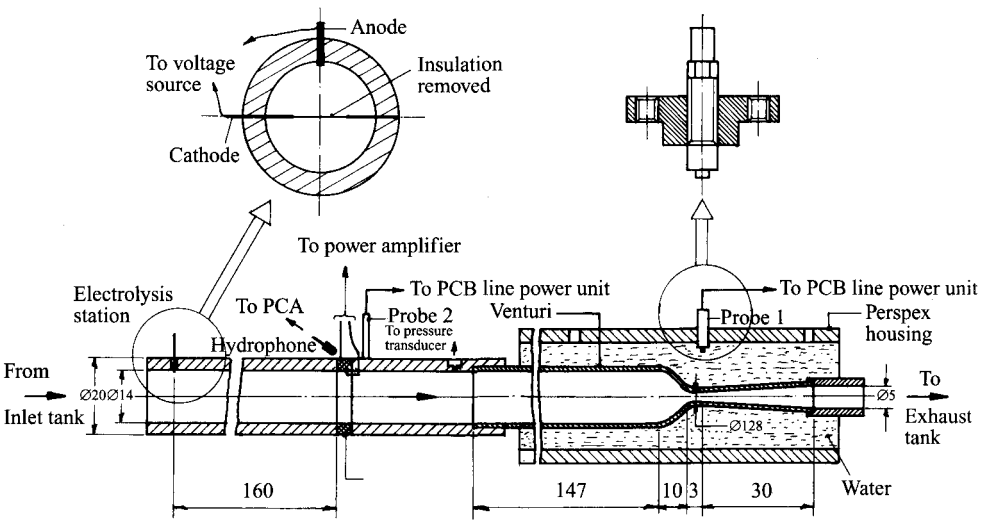


FIGURE 3. Details of the test section (dimensions in mm).

vacuum pump and the exhaust tank helped to maintain almost constant vacuum in the exhaust tank. Water flows from the inlet tank to the exhaust tank through a Perspex tube, the test section, and a flow-regulating valve. A small, monoblock pump unit is used to pump this water to the overhead tank from the sump. From this overhead tank, water could be siphoned to the inlet tank.

2.1. *Test section*

The most important part of the set-up is the test section (figure 3). It consists of three principal parts, namely a venturi, a piezoelectric transducer (UNM) and electrodes which are described in detail below.

Venturi: A venturi is required to create travelling bubble cavitation. It is made of glass to facilitate fabrication and visual observation of cavitation. The glass venturi consists of a long cylindrical inlet portion of length 147 mm and diameter 13 mm, followed by a smooth converging portion. The length of the converging portion is

https://doi.org/10.1017/S0022112096004223 Published online by Cambridge University Press

10 mm. The contraction ratio, defined as

$$C_c = \frac{A_{inlet}}{A_{throat}},$$

where A denotes area, is ≈ 100 with throat diameter being 1.28 mm. The approximate length of the throat is 3 mm. This is followed by a gradually opening smooth diffuser having an exit diameter of 5 mm.

It should be noted that the design of this venturi was done following the analysis of d' Agostino & Acosta (1983) and in particular the contraction ratio was intentionally kept very high. The high contraction ratio ensured a very low inlet velocity and laminar flow in the upstream tube but still produced cavitation at the throat. The typical Reynolds number at the inlet was about 1550. In the present experiments, laminar flow was a requirement since, unlike turbulence, laminar flow will interfere very little with initial bubble size due to a smaller effect on mass diffusion rates.

The test venturi being very delicate, it was protected by placing it in a Perspex housing. Two sides of the housing were made of flat windows which facilitated viewing and photography of cavitation near the throat. The housing was filled with water for improved acoustic transmission from the throat. It was found that reliable monitoring of cavitation events at the throat could be done by dipping a subminiature pressure transducer, PCB type 105A03 (designated as probe 1) in the water-filled Perspex housing as shown in figure 3. The details of the mounting of probe 1 are shown in the blow-up view in figure 3.

UNM: An acoustic pressure field is required upstream of the venturi to manipulate the nuclei as they pass through it. It is intended that these bubbles will undergo transient cavity motion under the influence of the ultrasonic pressure field. In the present geometry of the test section, the ultrasonic pressure field was suitably created by a piezoelectric transducer (PZT 5A) ring which has been termed an ultrasonic nuclei manipulator (UNM). The dimensions of this transducer were 20 mm o.d., 14 mm i.d., and 6 mm in length. The transducer was sandwiched between the ends of two Perspex tubes by epoxy resin (Araldite). The UNM was driven at the crystal resonant frequency, which was around 57 kHz and not at the system resonant frequency, which was estimated following the procedure of Ellis (1955) to be 34.25 kHz. This is because at the system resonant frequency, many small bubbles were observed to form on both upstream and downstream sides of the UNM which, when carried to the venturi throat, could act as sites for transient cavitation. It should be emphasized that the purpose of the UNM in the present experiments was to destroy nuclei and not to generate them.

Electrodes: As indicated earlier, in the present experiments, it was necessary to supply artificial nuclei to generate travelling bubble cavitation at the throat since, in its absence, the dominant type of cavitation was sheet cavitation in the diffuser. Electrolysis of water was employed as the means for producing artificial nuclei, a technique which has already been effectively utilized by Arakeri & Shanmuganathan (1985). In the present set-up, electrolysis bubbles were generated by mounting two electrodes in the Perspex tube upstream of the glass venturi and the UNM. The cathode consisted of a very fine (SWG 34) enamel-coated copper wire placed across the tube. Only the central part of this wire, where the enamel insulating coating was removed took part in hydrogen bubble production (see the blow-up view of electrodes in figure 3). The cathode was kept in cross-flow because previous trials with various electrode configurations revealed that bubbles were released most easily when in cross-flow. The diameter of the cathode had been selected to be very small so that the flow would

https://doi.org/10.1017/S0022112096004223 Published online by Cambridge University Press

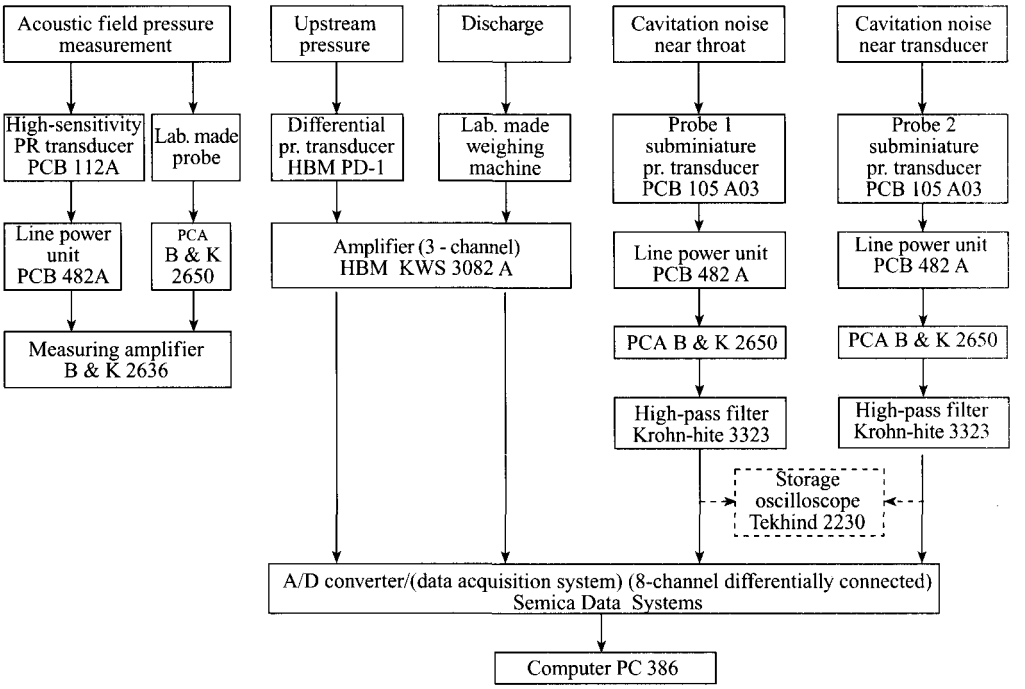


FIGURE 4. Block diagram of measuring side instrumentation. B & K denotes Bruel & Kjaer.

be least disturbed. The anode consisted of a copper terminal of diameter 1.32 mm which was flush mounted on the Perspex tube. Application of sufficient DC voltage to the electrodes resulted in hydrogen bubble evolution at the cathode. The distance between the site of nuclei generation (electrodes) and the site of hydrodynamic cavitation (venturi throat) was 430 mm and was selected as a compromise between the length required to avoid complete dissolution of hydrogen bubbles and to keep the influence of the UNM, which was mounted just downstream of electrolysis station, at the throat as small as possible.

The activity of nuclei near the UNM is of vital importance in the present experiments and needed to be monitored. Hence, another subminiature pressure transducer, PCB 105A03, denoted as probe 2 in figure 3, was mounted externally on the wall of the Perspex tube just downstream of the UNM using RTV silicone.

The instrumentation system can be broadly divided into the driving side instrumentation and the measuring side instrumentation.

The UNM is driven using a power amplifier (Bruel & Kjaer type 2713) and a sine random generator (Bruel & Kjaer type 1027). The driving frequency is noted in a frequency counter (HIL 2723). The pressure developed by this transducer is monitored in air by a commercial hydrophone (Bruel & Kjaer type 8103) whose output was first fed into a precision conditioning amplifier (PCA) (Bruel & Kjaer type 2650) and then to a measuring amplifier (Bruel & Kjaer type 2636). This monitoring facilitated tracking the resonant UNM crystal frequency. The electrolysis bubbles were generated by connecting the electrodes (figure 3) to a regulated DC voltage source.

The measurement side includes the instrumentation required for measuring the cavitation noise produced by bubbles, the upstream pressure and the flow rate; a block diagram of this instrumentation is shown in figure 4. The noise of collapsing

https://doi.org/10.1017/S0022112096004223 Published online by Cambridge University Press

bubbles associated with hydrodynamic cavitation near the venturi throat and acoustic cavitation within the UNM, if any, are picked up by probes 1 and 2 (figure 3). Both these probes are connected to the PCB line power unit. The output is fed first to PCA and then to a high-pass filter. The high-pass filter with a cut-off frequency of 99 kHz was used to suppress the probe output due to the pressure field created by the UNM. The filtered output was collected in a data acquisition system and was stored in a PC or directly monitored using a 100 MHz storage oscilloscope.

The reference pressure for computing cavitation number, etc. was measured by connecting a differential pressure transducer to a very small (1 mm in diameter) pressure tapping on the Perspex tube wall downstream of the UNM. The transducer was calibrated against a known height of a water column. The output of this pressure transducer is sent to an amplifier and finally to the data acquisition system. The flow rate was measured in an indirect, yet simple way. The exhaust tank is placed on a pan, which in turn is placed on a laboratory-made weighing machine. The output of the weighing machine was connected to an amplifier and finally to the data acquisition system. The use of a data acquisition system (DAS) was essential as the experiments were of transient nature.

3. Experimental methods and observations

Each experiment involved various operations and a brief description of a typical run is given below.

All the instruments were turned on about 30 minutes before starting the actual runs. Water from the overhead tank was siphoned to the inlet tank. If the water sample was required to be saturated, it was allowed to sit for about thirty-six hours. If partial degassing was required then water from the overhead tank was siphoned and sprayed into the inlet tank under vacuum. This increased the surface area of water and helped to get rid of gas easily. The amount of degassing could be controlled somewhat by varying the vacuum in the inlet tank, the amount of water sprayed and the time held under vacuum. This partially degassed sample was taken to MERL apparatus (modified Van Slykes' apparatus) for the measurement of the dissolved gas content. At this point, the water temperature was also noted.

Next the critical frequency of the UNM (typically around 57 kHz) was found and the exhaust tank was kept under vacuum (typically around 350–450 mm of mercury). Then the flow was started. The flow rate was controlled by a Teflon screw valve. If the objective of the run was to obtain the incipient or desinent (i.e. the beginning of cavitation and the disappearance of an established cavity) conditions or to study the effect of the UNM on bubbles, then the run was made for 40 s. Otherwise, for studying the effect of the UNM on cavitation occurrence at the venturi throat, the experiment was continued for 80 s. When required, the voltage applied to the electrodes for electrolysis was approximately 25 V and the driving voltage for the UNM was 4 V at 38 dB amplification using a power amplifier. Each of these runs (excepting incipient or desinent condition determination, where the UNM was inoperative) had a definite sequence of operating the UNM and electrolysis and this will become apparent when discussing results in figure 9. In each set of runs, two tests were done to ascertain the desinent conditions. Incipient and desinent conditions of cavitation were determined by observing cavitation near the venturi throat under the illumination of stroboscopic lighting.

In the data acquisition system, 4×10^5 (when run time is 40 s) or 8×10^5 (when run-time is 80 s) data points were stored per channel by scanning 10000 points per

https://doi.org/10.1017/S0022112096004223 Published online by Cambridge University Press

second. After processing and averaging, a smooth curve through 200 data points was finally used for obtaining cavitation number values from the outputs of the differential pressure transducer and the weighing machine. It may be noted that the probe outputs did not require any further processing.

During selected runs, photographs of cavitation at the venturi throat were taken with a dark background with the camera shutter kept open and a stroboscope operated in single flash mode.

Generally, at any flow rate and in the absence of electrolysis, the only type of cavitation observed was of the sheet type located just downstream of the venturi throat. This type of cavitation was characterized by a continuous, soft hissing sound. However, when electrolysis was turned on, travelling bubble type cavitation was readily noticed. The noise associated with this type of cavitation was quite distinct and consisted of a clearly audible individual, sharp sound. This distinction was also clearly apparent from the probe 1 output on a storage oscilloscope. When the UNM was made operative, the sound of collapsing bubbles could not be heard even with the aid of a stethoscope.

Near the UNM, when both electrolysis and the UNM are operative, faint sharp sounds could be heard clearly only with the aid of a stethoscope. However, with either electrolysis or UNM inoperative, this sound was not detectable.

As the UNM was a critical component of the test set-up, it was desirable to know the acoustic pressure field associated with it. It was not possible to measure this *in-situ* with commercial hydrophones due to their large size. Hence, the measurements were carried out using a separate set-up which is geometrically similar to the main one but with a miniature hydrophone which was designed and constructed in the laboratory for this purpose; the details are given in Chatterjee (1995). It was found that the maximum acoustic pressure obtained near the UNM was about 3.6 bar, which decreased to about 1.6 bar within a few cm from the UNM. These pressure amplitudes are sufficient to ensure transient cavity motions of electrolysis bubbles whose sizes are expected to be about 50–100 μm, based on an earlier study by Arakeri & Shanmuganathan (1985). It should be emphasized that knowledge of the exact size distribution of electrolysis bubbles or the acoustic pressure distribution is not critical in the present experiment. It was sufficient to ensure that the electrolysis bubbles were large enough to act as efficient nuclei for generating travelling bubble cavitation near the venturi throat. Similarly, when the UNM is operative, it was only required that the maximum acoustic pressure near the UNM be sufficiently large to drive electrolysis bubbles into transient cavity motion at the operating frequency. These requirements were adequately met by the procedures adopted here.

4. Results and discussion

Travelling bubble cavitation thresholds with added nuclei, namely the incipient and desinent cavitation numbers, designated σ_i and σ_d respectively, were measured and their averaged values for a saturated water sample are

$$\sigma_i = 1.05, \quad \sigma_d = 1.06.$$

However, for individual runs the σ_d value varied, for example, from 0.92 to 1.12. Here, σ is defined as

$$\sigma = \frac{p_o - p_v}{\frac{1}{2}\rho V_t^2}$$

https://doi.org/10.1017/S0022112096004223 Published online by Cambridge University Press

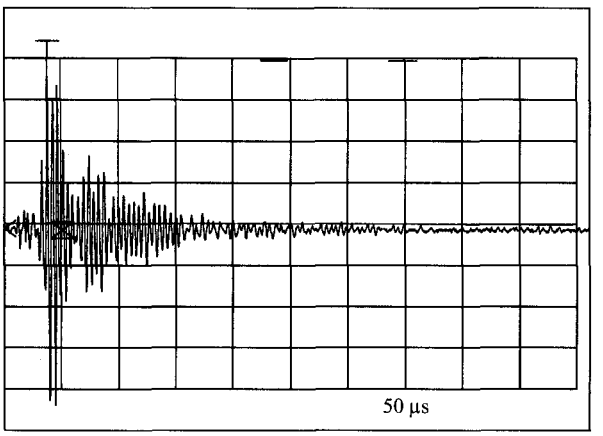


FIGURE 5. Probe-1 response depicting a single event from a collapsing cavitation bubble near the venturi throat as recorded on a storage oscilloscope.

where p_o and p_v are the upstream and vapour pressure respectively, V_t the throat velocity and ρ the density. p_o is obtained by measuring the static pressure upstream of the venturi throat and V_t is obtained from the flow-rate measurement. Classical arguments suggest that $\sigma_i \approx (-C_p)_{min}$, the minimum pressure coefficient, and this is particularly true when nuclei are being seeded (Kodama *et al.* 1979). An expression for the theoretical $(-C_p)_{min}$ value, obtained using Bernoulli's equation, is given by

$$(-C_p)_{min} = \frac{p_o - p_t}{\frac{1}{2}\rho V_t^2} = 1 - \left(\frac{d_t}{d_o}\right)^4$$

where d_o is the upstream diameter and p_t, d_t the pressure and diameter at the throat. In the present case $(-C_p)_{min} = 0.9904$. So, at least the averaged values of σ_i and σ_d are close to the $(-C_p)_{min}$ value as expected.

Next we describe results for cavitation near the venturi throat. Figure 5 shows the probe-1 response due to a single cavitation event as observed on the oscilloscope. The frequency associated with the initial part of the oscillation is approximately 250 kHz which matches reasonably well with the probe transducer resonant frequency as indicated by the manufacturer. So, this strongly suggests that shock waves are formed due to the collapse of individual cavitation bubbles downstream of the throat. This shock then drives the probe to resonance. Hence, it appears very difficult to obtain any quantitative information on the strength of bubble collapse from these measurements, even though the existence of such an event is definitely shown.

In figure 6 the probe output over a much longer time duration than in figure 5 is shown. One can clearly identify a large number of individual spikes, each one corresponding to a cavitation event. The results in figure 6 are associated with travelling bubble cavitation near the throat in the absence of the UNM. The dramatic effect of the UNM being made operative, under otherwise the same conditions, is illustrated in figure 7. From the fact that the individual spikes are completely suppressed, it is evident that travelling bubble cavitation was completely eliminated. What one sees in this figure is the pressure field associated with the UNM, the levels being reduced since the signals were high-pass filtered. The above observations are further supported from the photographs near the venturi throat in figures 8(*a*) and

https://doi.org/10.1017/S0022112096004223 Published online by Cambridge University Press

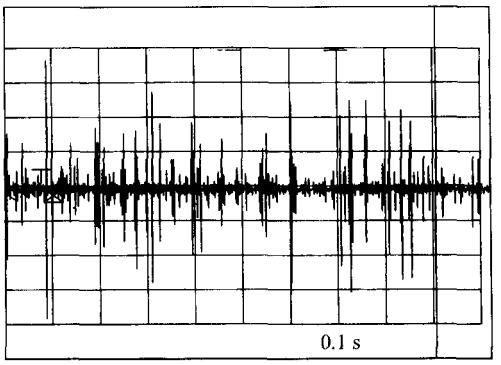


FIGURE 6. Probe-1 output at the venturi throat, when electrolysis is on but the UNM is inoperative, as recorded on a storage oscilloscope.

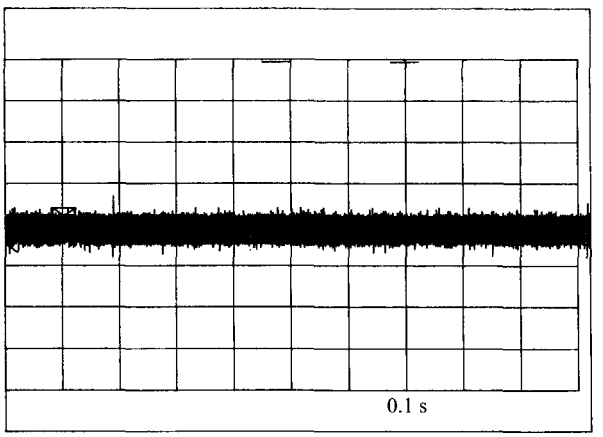


FIGURE 7. Probe-1 output at the venturi throat, when electrolysis is on and the UNM is operative, as recorded on a storage oscilloscope.

8(*b*). The travelling bubble cavitation as seen in figure 8(*a*) is made to completely disappear as the UNM is turned on, as is evident from figure 8(*b*).

More systematic studies of the probe-1 output under various experimental conditions were carried out using the data acquisition system. A typical result using the data acquisition system is shown in figure 9. The experiment was run for 80 s using a saturated water sample and for $\sigma - \sigma_d = -0.10$. As the σ_d value was obtained in the same experimental run the magnitude of $\sigma - \sigma_d$ gives a measure of the relative tension existing at the throat. The total duration of the run can be broadly divided into three time zones depending on the mode of operations performed in each time interval. In time zone 1 (0–13 s), both the electrolysis and UNM were switched off. The probe output in this zone is primarily due to the noise from the flowing water. In zone 2 (13–25 s), electrolysis was switched on but the UNM was still inoperative. This zone is characterized by a large number of individual spikes corresponding to travelling bubble cavitation noise. In zone 3 (25–55 s), electrolysis was continued and the UNM was turned on. This portion of the curve does not contain a single individual peak, thus clearly indicating the absence of any cavitation events taking place in this time interval. This once again shows the successful operation of the UNM. The widening of the signal band compared to zone 1 is due to the pressure field associated with the

https://doi.org/10.1017/S0022112096004223 Published online by Cambridge University Press

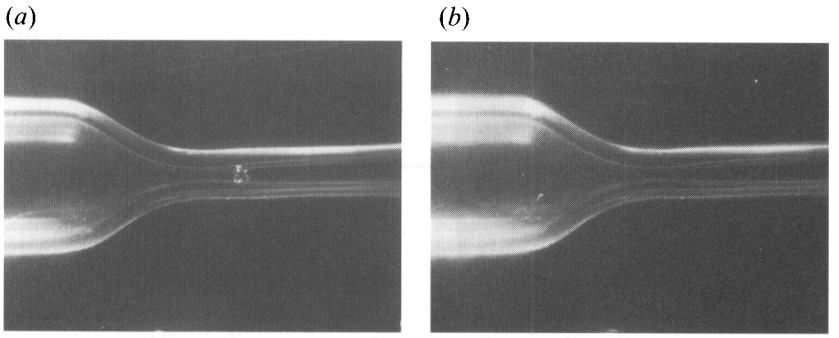


FIGURE 8. Photographs showing the cavitation event near the venturi throat: (*a*) the presence of cavitation when the UNM is inoperative, (*b*) the disappearance of cavitation when the UNM is operative.

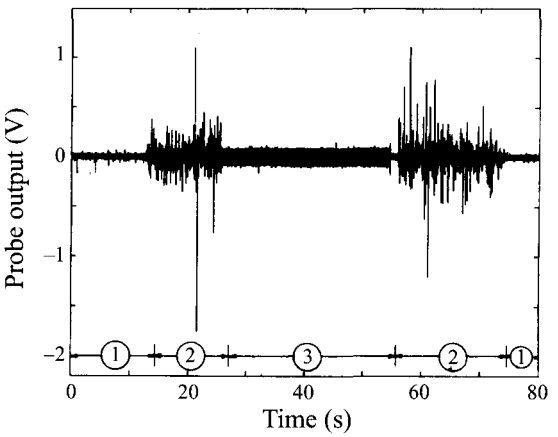


FIGURE 9. Probe-1 output from near the venturi throat for saturated water and for $(\sigma-\sigma_d) = -0.100$. Zone 1: neither electrolysis nor the UNM operative; zone 2: only electrolysis on; zone 3: both electrolysis and the UNM operative.

UNM itself. That the UNM is responsible for the elimination of travelling bubble cavitation near the throat is evident from the fact that as soon as the UNM is turned off, the individual spikes reappear (zone 2 after 55 s). It may be noted in this context that zone 2 of figure 9 bears striking similarity with the oscilloscope output in figure 6. This gives us confidence that the data acquisition system was capturing the essential features of the probe output.

Further studies were carried out to study the effectiveness of the UNM by varying some parameters like relative tension at the throat (reflected in the $\sigma - \sigma_d$ value) and the dissolved gas concentration in the liquid. It was established that the UNM was effective in controlling cavitation even with larger relative tension at the throat and was also effective with degassed water. Since all these results were qualitatively similar to those in figure 9, they are not presented here and may be found in Chatterjee (1995).

In most of the tests, including the ones mentioned above, the relative tension at the throat was limited to a value such that there was no sheet cavitation downstream of the throat. In figure 10, one set of results is presented where this restriction was relaxed. In this case, in the absence of seeding of bubbles (zone 1), only sheet cavitation was present. However, with seeding of nuclei (corresponding to zone 2) both travelling

https://doi.org/10.1017/S0022112096004223 Published online by Cambridge University Press

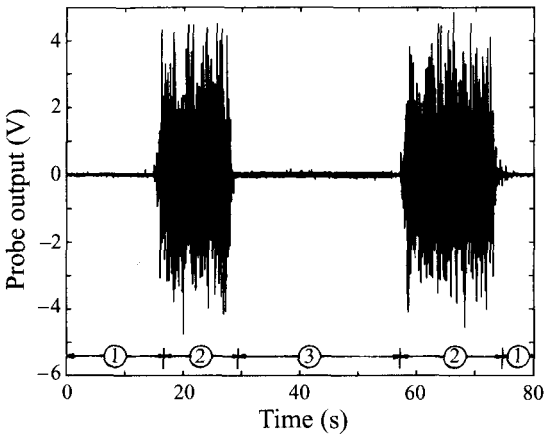


FIGURE 10. Probe-1 output from near the venturi throat for partially degassed water (gas content is 70% of saturation) and $(\sigma - \sigma_d) = -0.183$. Zone 1: neither electrolysis nor the UNM operative; zone 2: only electrolysis on; zone 3: both electrolysis and the UNM operative.

bubble cavitation and sheet cavitation were observed. The spikes in the output are clearly associated with travelling bubble cavitation since sheet cavitation does not seem to result in significant probe output as is seen from zone 1 of figure 10. When the UNM was made operative (zone 3), travelling bubble cavitation was completely suppressed as again evidenced by the probe output. However, it was visually observed that sheet cavitation still persisted. Therefore, this clearly indicates that the UNM is successful in eliminating travelling bubble cavitation but it is not at all effective in suppressing sheet cavitation. It is well known from the existing literature that sheet cavitation is associated with laminar separation (Arakeri & Acosta 1973) and hence its existence could be associated with local nuclei supply rather than the free-stream nuclei supplied from upstream. Further, from noise considerations, it is also well known that sheet cavitation is significantly quieter than travelling bubble cavitation and this is also observed in the present experiments as it is evident from figure 10, since when sheet cavitation was present during zone 1, the noise levels are of the same order as the background noise levels corresponding to zone 1 of figure 9. Therefore, the operation of the UNM for cavitation control is restricted in that it appears that the cavitation associated with free-stream nuclei only can be eliminated. Further work is required to examine whether sheet cavitation can also be controlled using the UNM; however, the need for controlling such cavitation is less as it is expected to have much reduced destructive capability.

It is necessary to bring out the underlying mechanism of cavitation control in order to extend its use and applicability beyond the laboratory conditions. A gas bubble will tend to dissolve in undersaturated or even saturated water (due to surface tension effects, Epstein & Plesset 1950) if no acoustic pressure field is imposed. If an acoustic pressure field is created, then the bubbles may coalesce, or may exhibit violent collapse, fragmentation and subsequent dissolution. Both these processes are capable of changing the nuclei size and number density and hence could play an important role in controlling hydrodynamic travelling bubble cavitation at the throat.

If a bubble undergoes transient cavity motion, one would expect cavitation noise associated with it. It has already been pointed out in the previous section that a faint audible sound was heard near the UNM and now more convincing evidence of acoustic cavitation near the UNM is presented in figures 11 and 12. The probe 2

https://doi.org/10.1017/S0022112096004223 Published online by Cambridge University Press

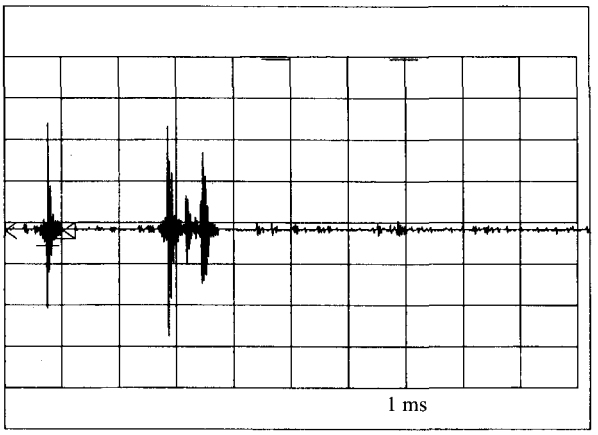


FIGURE 11. Probe-2 output from near the UNM, when electrolysis is on and the UNM is operative, as recorded on a storage oscilloscope.

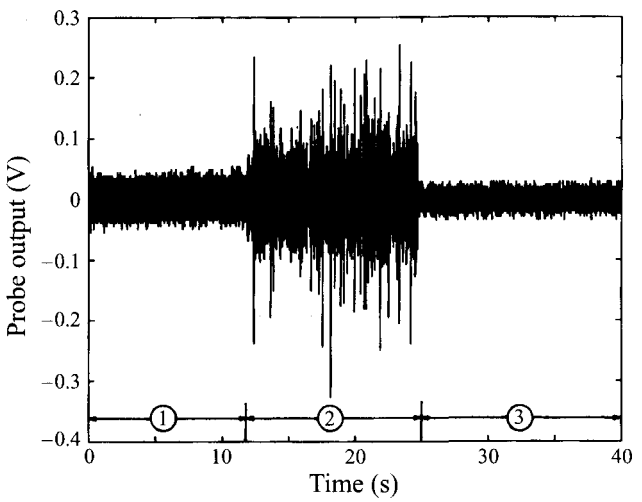


FIGURE 12. Probe-2 output from near the UNM for saturated water. Zone 1: only the UNM is operative; zone 2: both electrolysis and the UNM is operative; zone 3: only electrolysis is operative.

response corresponding to individual cavitation events is shown in the oscilloscope trace of figure 11. Figure 12 shows the probe 2 response as obtained from the data acquisition system. In figure 12 the run is divided into three time zones. In zone 1 (0–14 s), only the transducer was turned on, while electrolysis was kept off; no individual spike being seen in this time interval strongly suggests the absence of any transducer-induced cavitation. Such cavitation occurs only when electrolysis bubbles are seeded as in to time zone 2 (15–25 s), when both electrolysis and the UNM were made operative. It is only during this time that the individual spikes are seen. Zone 3 (25–40 s) shows the probe output with only electrolysis being on and again there is no sign of cavitation near the UNM as expected.

Attempts to detect the coalescence of electrolysis bubbles were made by careful observations with stroboscopic lighting and photographic means. Even though no clear-cut evidence for coalescence was found, slight alteration of nuclei number

https://doi.org/10.1017/S0022112096004223 Published online by Cambridge University Press

density due to coalescence cannot be ruled out. But there is no doubt that the dominant mechanism of cavitation control is associated with pre-cavitation of the nuclei due to the acoustic field produced by the UNM. Qualitatively this has been established; however, it would have been interesting to quantitatively measure how much the flow rate necessary to cavitate the water sample was increased by the presence of the UNM. We could examine this question only partially due to the appearance of sheet cavitation in the diffuser which limited the maximum flow rate. With the UNM on, we could increase the flow rate beyond inception by 5.6% before sheet cavitation appeared and by 7.5% before the venturi choked; travelling bubble cavitation was suppressed under these conditions. The estimated tension at the throat was respectively 2.2 kPa and 5.7 kPa and the nuclei sizes which have such threshold pressures and are in equilibrium with the upstream conditions ahead of the venturi are computed to be 5.4 μm and 3.8 μm respectively. Therefore, from the present observations we are certain that nuclei generated by electrolysis of size estimated to be greater than 50 μm are fragmented to at least 3.8 μm by the UNM. Note that, even with the use of more sophisticated techniques of direct nuclei measurement like laser light scattering or holography, it would be difficult to resolve the issue actually how small the nuclei are downstream of the UNM, since the resolutions of these techniques is around 5 μm and in particular it is difficult to distinguish between bubbles and particles at these sizes (Billet 1986). Therefore, to quantitatively resolve the issue, it would be necessary to develop an apparatus which can generate significantly larger tensions than possible with the venturi. One possibility is a spherical acoustic resonator, where, at the centre it is possible to generate large tensions but somehow it has to be integrated with the flow apparatus containing the UNM.

Comparing the results from probe-1 and probe-2 outputs as shown in figures 9 and 12, it appears that the noise levels associated with hydrodynamic cavitation and acoustic cavitation events are similar. However, it should be pointed out that there is no actual basis for comparing the two results since probe 2 was directly mounted on the wall of the Perspex tube and probe 1 was mounted on a perspex housing filled with water (see figure 3). A more realistic comparison between the noise levels from the two types of cavitation can be obtained by computing the maximum radius(R_{max}) attained by a nucleus in the two pressure fields. This follows from the computations of Fitzpatrick & Strasberg (1956) who have shown that the absolute cavitation noise levels scale like R_{max}^3. Since only the growth phase of bubbles was of interest, a simplified form of the Rayleigh–Plesset (RP) bubble dynamics equation (Plesset & Prospretti 1977) was solved. The RP equation, with standard notation, used here is

$$\rho(R\ddot{R} + \tfrac{3}{2}\dot{R}^2) = \left(p_v + p_{go}\left(\frac{R_o}{R}\right)^3 - \frac{2\sigma}{R} - P(t)\right)$$

where the left-hand-side terms refer to the inertial contributions from the bubble motion and the right-hand side contains the various pressure terms, i.e. vapour pressure, gas pressure (assumed to follow isothermal law), surface tension and the driving pressure.

For the acoustic case, $P(t)$ can be expressed as

$$P(t) = P_b - P_A \sin \omega t$$

where P_b is the ambient pressure ($\approx$ 1 bar), P_A is the acoustic pressure amplitude taken to be 2.64 bar which is the average value of the results obtained from acoustic pressure measurements near the UNM, and $\omega = 2\pi f$ where f = 57 kHz in the present

https://doi.org/10.1017/S0022112096004223 Published online by Cambridge University Press

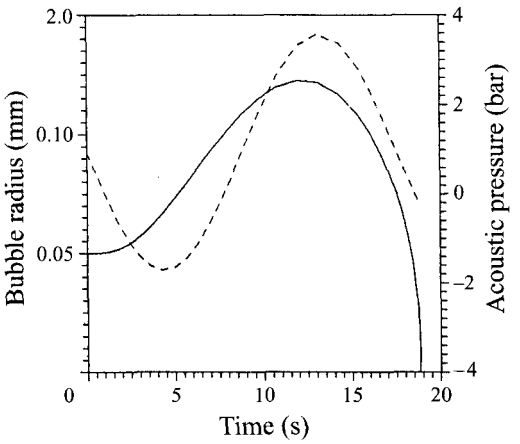


FIGURE 13. Computed bubble motion (—) corresponding to the acoustic pressure field (- - -) created by the UNM.

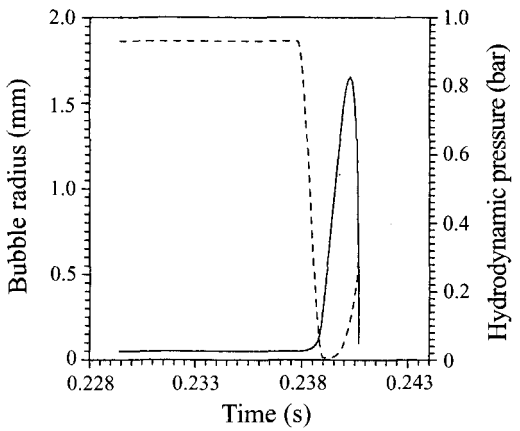


FIGURE 14. Computed bubble motion (—) corresponding to the hydrodynamic pressure field (- - -) for $(\sigma - \sigma_d) = -0.146$.

case. For the hydrodynamic case, $P(t)$ is the pressure sensed by a nucleus as it passes through the venturi. This pressure can be computed by knowing the spatial pressure distribution and the local velocity of the nucleus which is assumed to be the same as that of the liquid. Both these quantities can be obtained by using the Bernoulli equation for the measured flow rate. The acoustic and hydrodynamic pressure fields as experienced by a typical nucleus and the corresponding bubble growth and collapse phases, as computed using the RP equation, are shown in figures 13 and 14. From these figures, it is clear that the maximum radius for the hydrodynamic case (≈ 1.65 mm) is an order of magnitude larger than that for the acoustic case (≈ 0.123 mm) and from the results of Fitzpatrick & Strasberg (1956) we may expect substantially reduced noise levels in the acoustic case.

Another measure of the destructive capability of a cavitation bubble is the potential energy of the bubble at its maximum radius, denoted by PE_M and given by

$$PE_M = \tfrac{4}{3}\pi R_{max}^3 P_c$$

where P_c is the collapse pressure and R_{max} is the maximum bubble radius. The ratio

https://doi.org/10.1017/S0022112096004223 Published online by Cambridge University Press

of the potential energies of the acoustic and hydrodynamic fields obtained from the computations is

$$\frac{(PE_M)_{acoustic}}{(PE_M)_{hydrodynamic}} = \left(\frac{0.1225}{1.65}\right)^3 \times \frac{3.31}{0.53455} \approx 0.0025.$$

This value, being very small, shows that there can be a substantial gain by controlling hydrodynamic ('macro') cavitation through acoustic ('micro') pre-cavitation. The exact magnitude of the above ratio could be different if additional effects like multibubble growth, the effect of the wall, and the asymmetry of the bubble shape, as discussed by Chahine & Shen (1986), are considered; however, the order of magnitude is not expected to be substantially different.

From cavitation noise considerations, another significant aspect from computed bubble motion can be highlighted. The collapse time of a bubble in acoustic cavitation is of the order of 10 μs and that in hydrodynamic cavitation is of the order of 0.1 ms. We know from the results of Fitzpatrick & Strasberg (1956) that the maximum in noise spectrum is observed at $f_n\tau_c \approx 0.4$, where f_n is the peak frequency of the noise spectrum and τ_c is the collapse time of a bubble. So the dominant frequencies in the noise spectrum in the case of ultrasonic cavitation are expected to be considerably higher than the values expected in the case of hydrodynamic cavitation. Hence the former will be attenuated much faster in the liquid and this can be considered as an additional gain.

Before summarizing our results we would like to consider the potential application of the present technique. From the start we had two applications in mind: one involves liquid-sodium-cooled Fast Breeder Reactors (FBR) and second is control valves. In the first application, avoidance of cavitation is quite important since it is proposed to detect voidage from boiling in the core using acoustic means. The UNM could be placed in any convenient location in the coolant pipe and the fact that coolant in the FBR operates in a closed system is an added advantage since the coolant will then pass through the UNM repeatedly. In control valves involving certain applications noise reduction has become an important issue and in this case the UNM could be placed in the duct leading to the control valve. It is clear that in any application, UNM will consume additional power and here we can point out that a well-tuned acoustic transducer system can generate large-amplitude pressure fields with very low power consumption. For example, in our present experiments the UNM consumed only about 1 W of power (actually measured) corresponding to a power density of 0.5 W cm^{-2}, which may be a more significant parameter in considering scale-up. Thus, the added energy cost, unless involving a very large system, should not be significant. In addition, it is necessary to consider the potential risk from the secondary acoustic cavitation near the UNM. We have already demonstrated using the bubble dynamics equation that the noise levels from the secondary cavitation are expected to be significantly lower than from the primary hydrodynamic cavitation; also the dominant frequencies are predicted to be in the higher-frequency range. There is also the possibility of tailoring the UNM frequency to a particular application such that the frequency range of secondary cavitation noise is not annoying or interfering. It is entirely possible that the UNM parts may be subjected to cavitation erosion; however, since it will be placed in a convenient location, replacement should not pose major difficulties. Therefore, on the whole, it can be argued that the gains due to primary hydrodynamic cavitation reduction in a practical device should outweigh the

https://doi.org/10.1017/S0022112096004223 Published online by Cambridge University Press

added energy cost and the risk of secondary acoustic cavitation from operating the UNM.

5. Summary

The present study is aimed at exploring the possibility of using ultrasonics for hydrodynamic cavitation control. The basic test set-up required for this consisted of a glass venturi to generate hydrodynamic cavitation, a piezoelectric transducer to act as an ultrasonic nuclei manipulator (UNM) and an electrolysis station to ensure a copious supply of free-stream nuclei. Pressure pulses generated from the collapse of cavitation bubbles were monitored with a miniature pressure transducer mounted just above the venturi throat. The UNM, in the present experiments, consisted of a ring piezoelectric transducer which was mounted just downstream of the electrolysis bubble-generating unit. This transducer was driven at the crystal resonant frequency of about 57 kHz with a power level to yield an average acoustic pressure amplitude of about 2.64 bars near the UNM. Hydrodynamic cavitation control was demonstrated as follows: first travelling-bubble type hydrodynamic cavitation was generated at the throat by having sufficient flow rate through the venturi with electrolysis bubbles being seeded, and then the UNM was turned on and the resulting influence was noted. The dramatic effect of the complete disappearance of existing hydrodynamic cavitation at the throat was clearly observed (both visually and from the transducer output) with the UNM on. As soon as the UNM was turned off, cavitation reappeared. Thus, the concept of hydrodynamic cavitation control through ultrasonics was clearly demonstrated. Monitoring of the phenomena near the UNM confirmed the existence of acoustic pre-cavitation from nuclei which were electrolysis bubbles. Even though the control of hydrodynamic cavitation achieved here is at the expense of acoustic cavitation, it is shown, through the solution of the bubble dynamics equation, to be a significant advantage.

This work formed a part of the MSc (Engng) thesis of the first author. We would like to thank A. Giri and S. V. Raoot for their assistance in conducting the experiments and D. Govindraju for expert fabrication of the experimental components.

REFERENCES

APFEL, R. E. 1981 Acoustic cavitation. *Meth. Exptl Phys.* **19**, 355–411.

ARAKERI, V. H. & ACOSTA, A. J. 1973 Viscous effects in the inception of cavitation on axisymmetric bodies. *Trans. ASME J. Fluids Engng* **95**, 519–527.

ARAKERI, V. H. & CHAKRABORTY, S. 1990 Studies towards potential use of ultrasonics in hydrodynamic cavitation control. *Current Sci.* **59**, 1326–1333.

ARAKERI, V. H. & SHANMUGANATHAN, V. 1985 On the evidence for effect of bubble interference on cavitation noise. *J. Fluid Mech.* **159**, 131–150.

BARGER, J. E. 1964 Thresholds for acoustic cavitation. *Acoustic Research Laboratory, Harvard University Tech. Mem. 57.*

BILLET, M. 1986 Importance and measurement of cavitation nuclei. In *Advancements in Aerodynamics, Fluid Mechanics, and Hydraulics* (ed. R. E. A. Arndt, H. G. Stefan, C. Farell, and S. M. Peterson), pp. 967–988. ASCE.

CHAHINE, G. L. & SHEN, Y. T. 1986 Bubble dynamics and cavitation inception in cavitation susceptibility meters. *Trans. ASME J. Fluids Engng* **108**, 444–452.

CHATTERJEE, D. 1995 Towards the concept of hydrodynamic cavitation control. MSc (Engng) Thesis, Indian Institute of Science, Bangalore, India.

https://doi.org/10.1017/S0022112096004223 Published online by Cambridge University Press

D'AGOSTINO, L. & ACOSTA, A. J. 1983 On the design of cavitation susceptibility meters. *20th American Towing Tank Conf., Hoboken, NJ*, pp 1–19.

ELLIS, A. T. 1955 Production of accelerated cavitation damage by an acoustic field in a cylindrical cavity. *J. Acoust. Soc. Am.* **27**, 913–921.

EPSTEIN, P. S. & PLESSET, M. S. 1950 On the stability of gas bubbles in liquid-gas solutions. *J. Chem. Phys.* **18**, 1505–1509.

FITZPATRIC, H. M. & STRASBERG, M. 1956 Hydrodynamic sources of sound. *1st Symp. Naval Hyd., ONR, Washington DC*, pp. 241–280.

FLYNN, H. G. 1964 Physics of acoustic cavitation in liquids. *Phys. Acoust.* **1B**, 58–172.

FLYNN, H. G. & CHURCH, C. C. 1984 A mechanism for the generation of cavitation maxima by pulsed ultrasound. *J. Acoust. Soc. Am.* **76**, 505–512.

FLYNN, H. G. & CHURCH, C. C. 1988 Transient pulsations of small gas bubbles in water. *J. Acoust. Soc. Am.* **84**, 985–998.

HARRISON, M. 1952 An experimental study of single bubble cavitation noise. *J. Acoust. Soc. Am.* **24**, 776–782.

HOLL, J. W. 1970 Nuclei and cavitation. *Trans ASME J. Basic Engng* **92**, 681–688.

KNAPP, R. T., DAILY, J. W. & HAMMITT, F. G. 1970 Cavitation. *McGraw-Hill.*

KODAMA, Y., TAMIYA, S., TAKE, N. & KATO, H. 1979 The effect of nuclei on the inception of bubble and sheet cavitation on axisymmetric bodies. *ASME Intl Symp. on Cavitation Inception, New York* (ed. W. M. B. Morgan & B. R. Parkin), pp. 75–86.

NYBORG, W. L. & HUGHES, D. E. 1967 Bubble annihilation in cavitation streamers. *J. Acoust. Soc. Am.* **42**, 891–894.

PLESSET, M. S. & PROSPERETTI, A. 1977 Bubble dynamics and cavitation. *Ann. Rev. Fluid Mech.* **9**, 145–185.

https://doi.org/10.1017/S0022112096004223 Published online by Cambridge University Press